Recent Ka-Band Weather Statistics for Goldstone and Madrid

L. J. Harcke, P. F. Yi, and M. K. Sue
Communications Systems and Research Section

H. H. Tan
Communications Systems and Research Section
and
University of California, Irvine

Ka-band (32-GHz) radio communication links are more adversely affected by atmospheric noise temperature than X-band (8.4-GHz) or S-band (2.9-GHz) links. As a result, the strategy for telecommunications between a spacecraft employing Ka-band and the Deep Space Network is necessarily different from that employed at the lower frequencies. To aid in the development of new communication strategies, several years of 31.4-GHz water vapor radiometer data from the Goldstone and Madrid sites were reduced. Renewal theory was employed to examine the failure and recovery statistics of these Ka-band weather-dependent links.

I. Introduction

The Deep Space Network has been developing Ka-band (32-GHz) communications systems for future deep-space missions. X-band (8.5 GHz) has been the communication frequency for most deep-space missions for many years. Ka-band, however, has significant link advantage over X-band because the higher frequency allows the spacecraft to focus the transmitted RF energy in a smaller beam. For the same spacecraft antenna size and transmitter output power, the potential link performance gain is equal to the frequency ratio squared, or about 12 dB. This advantage can translate to a higher data rate, smaller antenna size, lower mass, lower DC power consumed on board the spacecraft, or a combination of these. A number of factors adversely affect Ka-band link performance, thereby reducing the achievable advantage over X-band. These factors include lower transmitter efficiency, higher receiver noise temperature, and more severe atmospheric effects. To overcome these technological challenges, the Telecommunications and Mission Operations Directorate (TMOD) has funded or augmented the development of key Ka-band technologies: a small deep-space transponder with Ka-band downlink capability and an efficient Ka-band solid-state power amplifier for the spacecraft, and a 34-m-diameter Ka-band beam-waveguide ground antenna, associated pointing schemes, and a low-noise front end. In concert with technology development, TMOD has funded system studies to develop new operational concepts for Ka-band to mitigate the adverse weather effects and other operational issues. This two-prong approach will improve Ka-band link performance and benefit future missions, including the Pluto Fast Flyby and the New Millennium Program, both of which are currently planning to use Ka-band communication systems.

A new operational concept is needed for Ka-band because it is much more susceptible to adverse atmospheric effects. Deep-space communications links using S- or X-band are typically designed to achieve from 90- to 95-percent link availability. However, providing such a high link availability for a Ka-band link requires a large link margin, hence a significantly reduced data rate, and ultimately may result in a design that is not optimum in the sense of maximizing the total telemetry data volume. The excess margin in the high availability link could be used to achieve a higher data rate. This point is illustrated in Figs. 1 and 2, which give the relative net telemetry data volumes as a function of the designed link availabilities for X-band and Ka-band for a candidate mission to Pluto. The lower data rate needed to ensure higher link availability results in a lower overall number of data bits successfully received on the ground. Ka-band weather models published in an JPL internal document, referred to herein as 810-5,[1] were used in calculating the relative data volume shown in the figures. These show that the optimal link availability for Goldstone is around 80 percent for Ka-band and 90 percent for X-band. This suggests that a possible operational strategy for Ka-band is to employ a retransmission scheme and operate the link at a lower link availability than X-band.

Ka-band weather statistics are key to the development of an operational concept [1]. Ka-band water vapor radiometers (WVRs) operating at 31.4 GHz have been installed at the Madrid and Goldstone Deep Space Communication Complexes (DSCCs) to collect atmospheric noise temperature data. These data have been reduced to generate Ka-band atmospheric noise temperature ("weather") statistics, which can be used to design telecommunications links for future missions; develop Ka-band operational concepts; and understand their operational implications, such as throughput efficiency and data latency. This article documents the Ka-band weather statistics for Madrid, based on WVR data collected between August 1990 and June 1993,[2] and for Goldstone, based on WVR data between October 1993 and September 1994.[3]

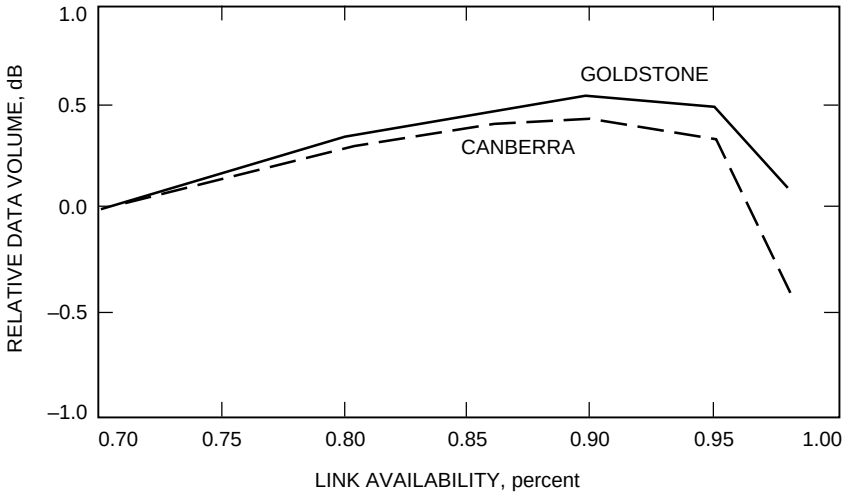

Fig. 1. Relative net telemetry data volume: 34-m high-efficiency antenna, X-band, Pluto Flyby, 25-deg elevation angle.

[1] S. D. Slobin, "DSN Telecommunications Interfaces—Atmospheric and Environmental Effects," *Deep Space Network/Flight Project Interface Design Handbook*, 810-5, Rev. C (internal document), vol. 1, ch. TCI-40, Jet Propulsion Laboratory, Pasadena, California, May 1992.

[2] S. J. Keihm, B. L. Gary, and S. J. Walter, *Spain 31 GHz Observations of Sky Brightness Temperatures: June 1990–June 1992*, JPL D-10710 (internal document), Jet Propulsion Laboratory, Pasadena, California, October 1992.

[3] S. J. Keihm, "Goldstone 31.4 GHz WVR Statistics, October 93–July 94," JPL Interoffice Memorandum 3833-94-410/SJK (internal document), Jet Propulsion Laboratory, Pasadena, California, August 1994.

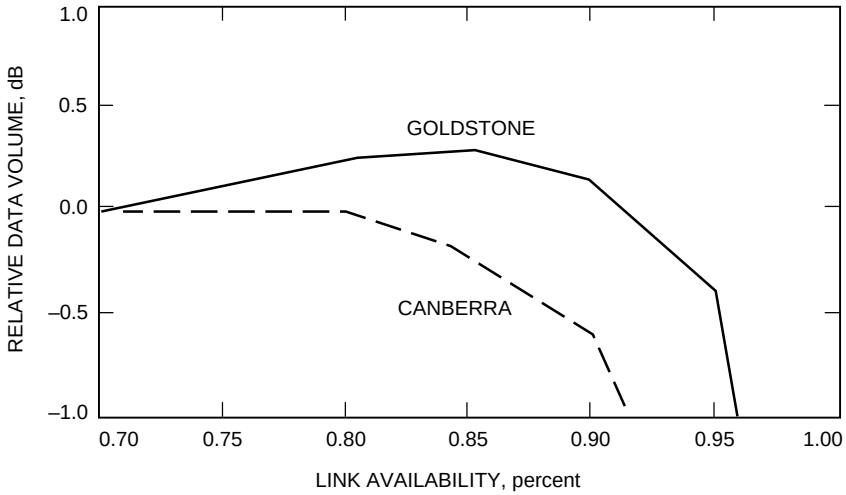

Fig. 2. Relative net telemetry data volume: 34-m beam-waveguide antenna, Ka-band, Pluto Flyby, 25-deg elevation angle.

II. Weather Statistics

The atmospheric noise temperature (which does not include cosmic background noise) at any given time t can be denoted by the stochastic process $\mathbf{T}(t)$. The normalized histogram or probability density function $f_T(T)$ is easily derived from radiometer data by binning the radiometer output in 1-K increments and normalizing the resulting histogram as shown in Figs. 3 and 4. Integrating this density function gives the cumulative distribution function for weather,

$$F_T(T) \equiv P\{\mathbf{T} \leq T\} \tag{1}$$

$$= \int_0^T f_T(T')\, dT' \tag{2}$$

shown in Figs. 5 and 6.

For reference, the cumulative distribution function from 810-5 is plotted as well.[4] Note the data for Goldstone show a higher average atmospheric noise temperature than those reported in 810-5, while the Madrid data show a lower average atmospheric noise temperature than those in 810-5. The 810-5 models are based on April–June 1984 Madrid data [2] and July 1984–December 1985 Canberra data [3]. The difference between the Madrid data and 810-5 was noted previously by Keihm et al. and was attributed to yearly variations in the atmosphere and different data processing algorithms.[5] These more recent data sets in this analysis are believed to be accurate to ±1 K.

Historically, percentage weather thresholds have been used for space mission planning. The percentage weather threshold is calculated by inverting the atmospheric noise temperature cumulative distribution function. For example, the 90-percent weather threshold is

[4] S. D. Slobin, op cit.

[5] S. J. Keihm, B. L. Gary, and S. J. Walter, op cit.

$$T_{90} = F_T^{-1}(0.9) \tag{3}$$

meaning that 90 percent of the time the atmospheric noise temperature will be at or below T_{90}. This is often called 90-percent weather availability. A space communication link is typically designed to have from 90- to 95-percent weather availability.

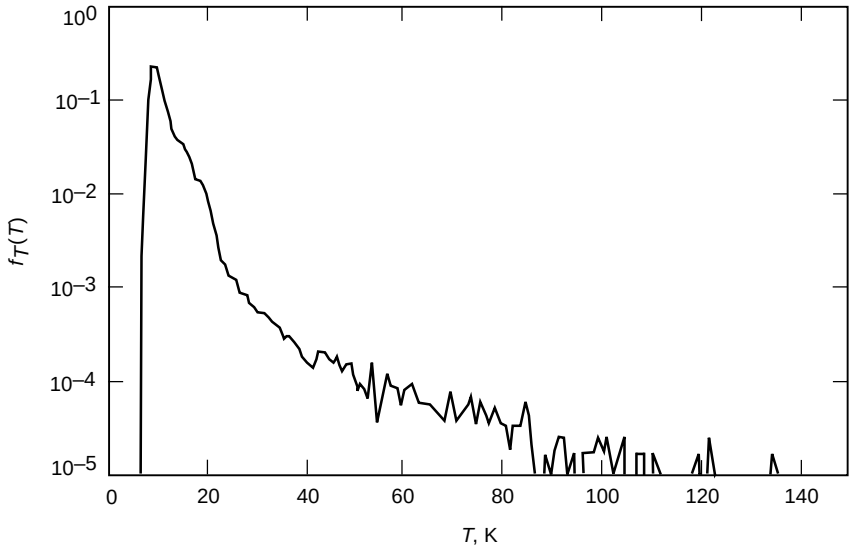

Fig. 3. Goldstone Ka-band 90-deg elevation atmospheric noise temperature probability density function—October 1993 through September 1994 average.

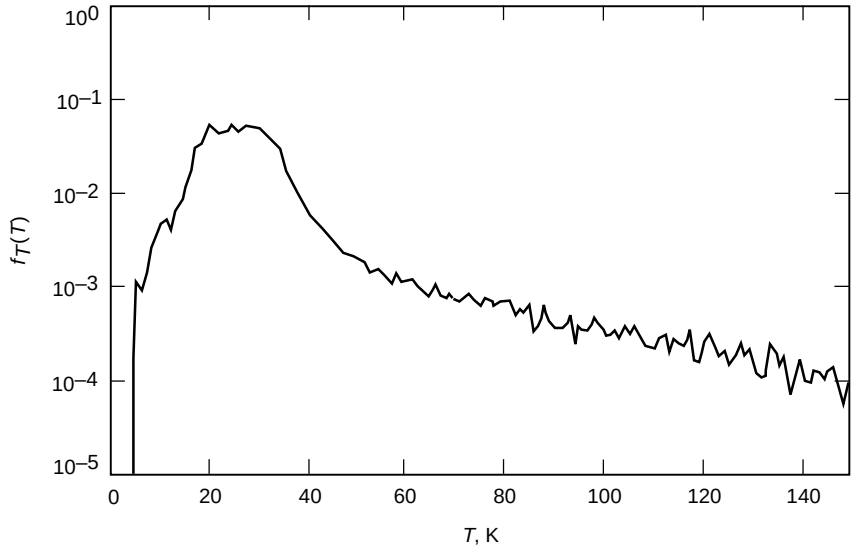

Fig. 4. Madrid Ka-band 30-deg elevation atmospheric noise temperature probability density function—August 1990 through June 1993 average.

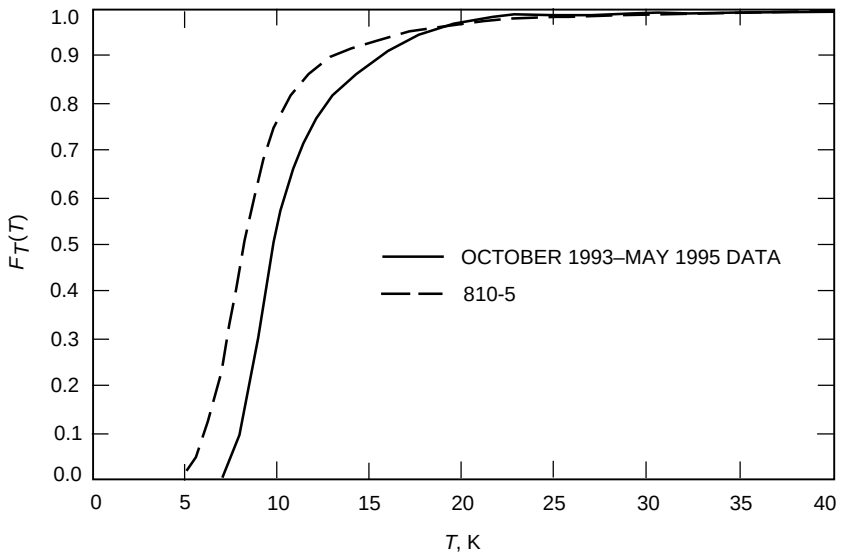

Fig. 5. Goldstone Ka-band 90-deg-elevation atmospheric noise temperature cumulative distribution function—October 1993 through September 1994 average.

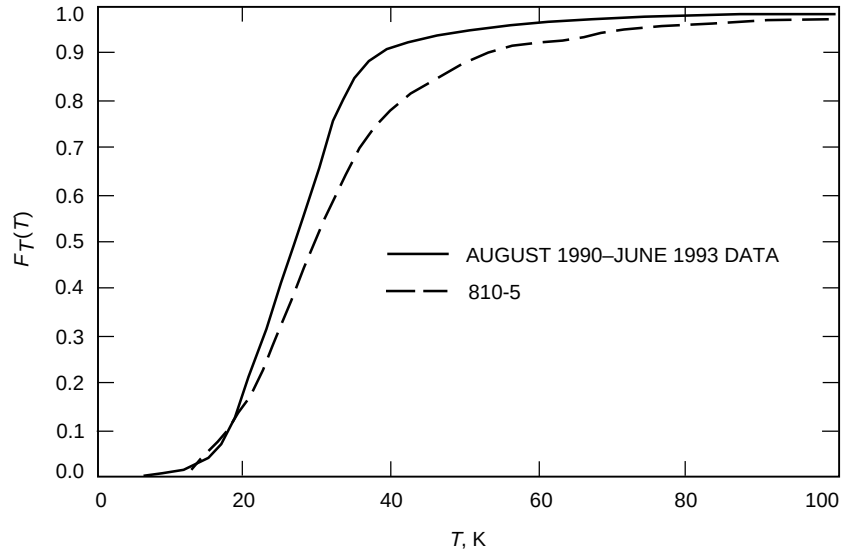

Fig. 6. Madrid Ka-band 30-deg-elevation atmospheric noise temperature cumulative distribution function—August 1990 through June 1993 average.

III. Link Reliability

Atmospheric noise temperature affects link reliability since an outage occurs whenever the noise temperature exceeds the link design threshold, as shown in Figs. 7 and 8. As the atmospheric noise temperature crosses and recrosses the link design threshold as a function of time, a series of uptime, $\mathbf{u}_i$, and downtime, $\mathbf{d}_i$, intervals is generated, as shown in Fig. 9. An uptime is defined as a period when the atmospheric noise temperature is below the communications link design threshold, while a downtime is defined as a period when the atmospheric noise temperature is above the communications link design

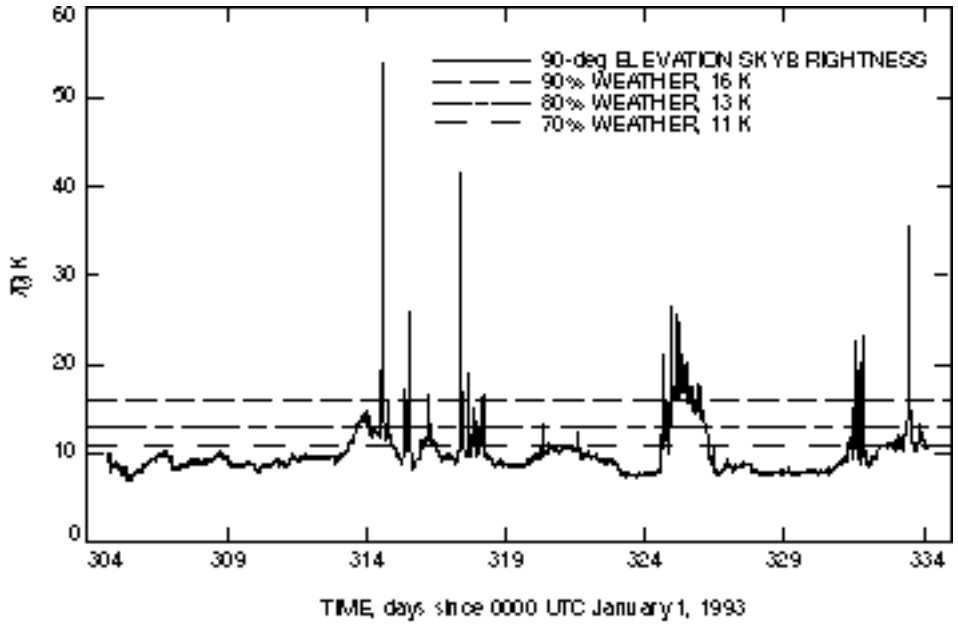

Fig. 7. Goldstone 31.4-GHz atmospheric noise temperature at a 90-deg elevation

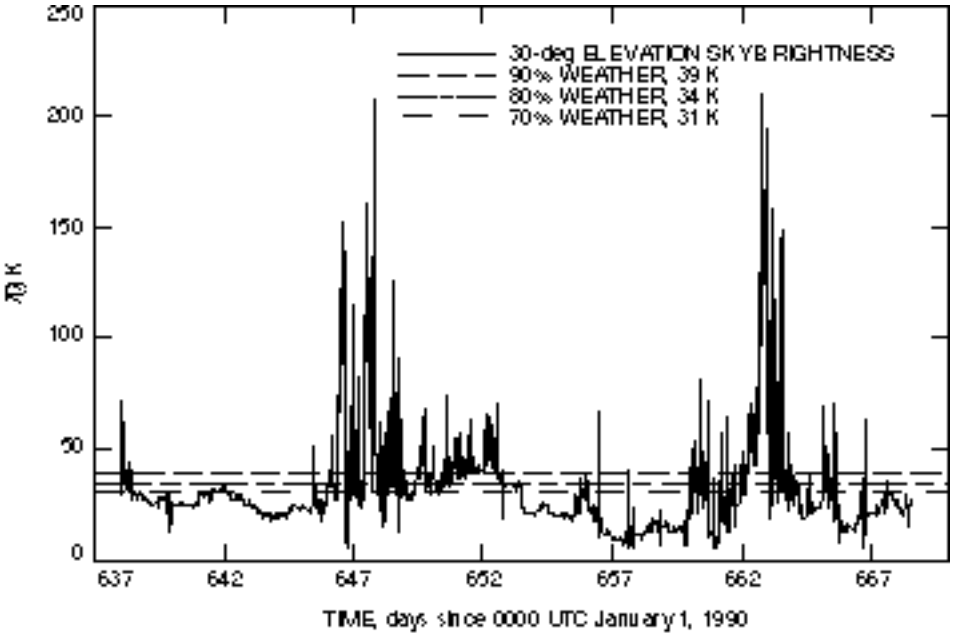

Fig. 8. Madrid 31.4-GHz atmospheric noise temperature at a 30-deg elevation

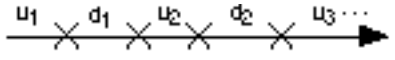

Fig. 9. Uptime and downtime

threshold. It is of interest to determine the distribution of these intervals. Assuming that $\{\mathbf{u}_i\}$ and $\{\mathbf{d}_i\}$ are independent sequences, we can investigate each series individually, as shown in Fig. 10. Further, assuming that each sequence $\{\mathbf{u}_i\}$ and $\{\mathbf{d}_i\}$ is independent and identically distributed, we can use renewal theory [4] to investigate the properties of the link. Bringing up the communication link at time t_0 and finding ourselves in the uptime or downtime interval $\mathbf{c}_i \in \{\mathbf{u}_i, \mathbf{d}_i\}$, we are interested in the distribution of the residual lifetime $\mathbf{w}$ of this event, as shown in Fig. 11 [4]. The random variable

$$\mathbf{w} = \mathbf{t}_1 - t_0 \tag{4}$$

has the probability density function

$$f_w(w) = \frac{1}{\eta_c}[1 - F_c(w)] \tag{5}$$

where

$$\eta_c = E\{\mathbf{c}_i\} = \int_0^\infty [1 - F_c(c)]\, dc \tag{6}$$

and

$$F_c(w) = P\{\mathbf{c}_i \leq w\} \tag{7}$$

$$= \int_0^w f_{c_i}(w')\, dw' \tag{8}$$

The probability density function $f_c(c)$ is computed from the data directly for a given atmospheric noise temperature threshold.

The remaining time in the interval between time t_0 and t_1 is known as the residual lifetime and is described by the reliability function

$$R_w(t) = P\{\mathbf{w} > t\} \tag{9}$$

$$= 1 - F_w(t) \tag{10}$$

$$= 1 - \int_0^t f_w(t')\, dt' \tag{11}$$

while the mean time to failure (if $\mathbf{c}_i = \mathbf{u}_i$) or mean time to recovery (if $\mathbf{c}_i = f\mathbf{d_i}$) is given by

$$\eta_w = E\{\mathbf{w}\} = \int_0^\infty w\, f_w(w)\, dw \tag{12}$$

$$= \int_0^\infty R_w(t)\, dt \tag{13}$$

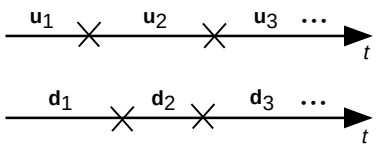

Fig. 10. Uptime and downtime independence.

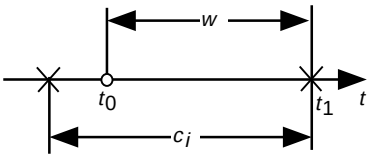

Fig. 11. Residual lifetime [4].

Figures 12 through 15 give the weather reliability function $R_w(t)$ for $\mathbf{u}_i$ and recovery function $F_w(t)$ for $\mathbf{d}_i$ for both Goldstone and Madrid. Table 1 shows the mean time to failure (MTF) and mean time to recovery (MTR) statistics for weather availability percentages of 70, 80, and 90, taken from the data sets in Figs. 5 and 6. This information can be a useful tool to the mission designer. For example, when choosing a link design with 80-percent weather availability, one would expect an MTF of 58.5 h after the beginning of a track at Goldstone. Choosing a weather availability of 90 percent increases the MTF to 89 h. Some mission phases could tolerate more weather outages than others. During routine interplanetary cruise, fields and particles science instrument data and engineering data could be telemetered at higher rates, with outages accepted as they occur. For critical mission events, such as trajectory correction maneuvers, encounters, planetary orbit insertions, or landings, telemetry weather outages would not be tolerated. The link threshold, and hence the data rate, could be set accordingly.

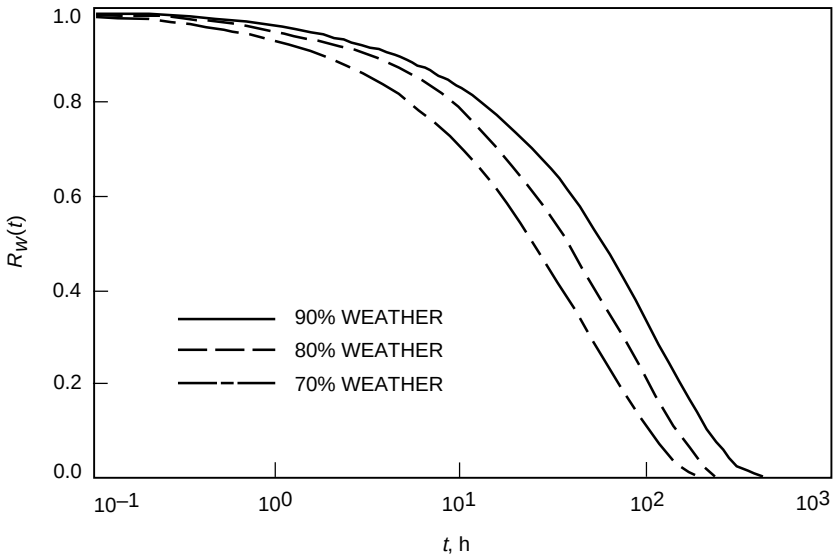

Fig. 12. Goldstone weather link reliability.

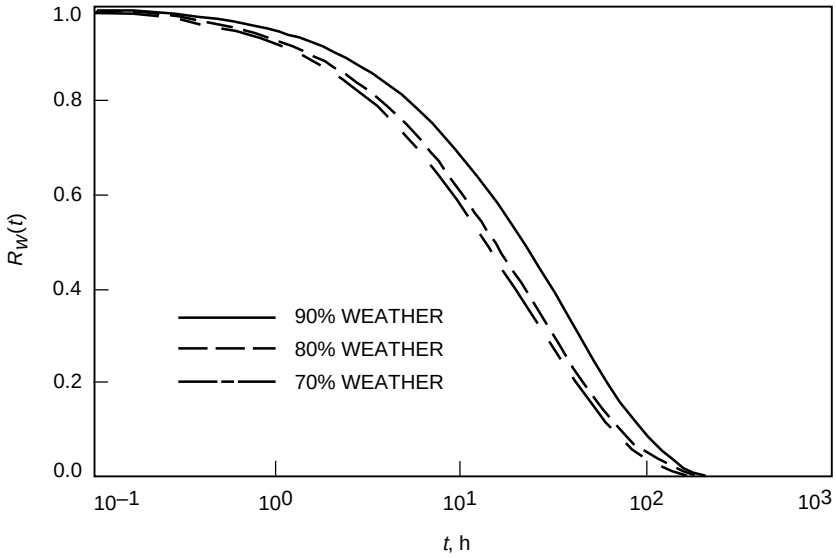

Fig. 13. Madrid weather link reliability.

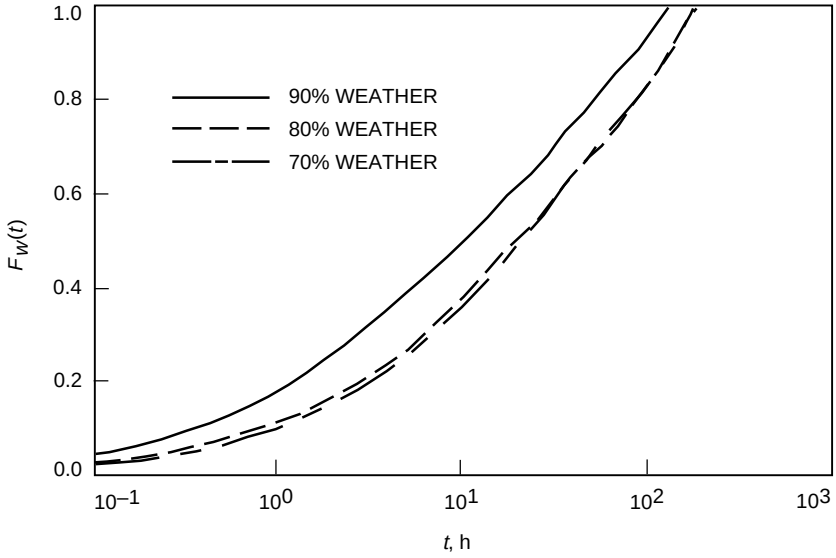

Fig. 14. Goldstone weather link recovery.

IV. Future Directions

It is well known that the seasonal mean atmospheric noise temperature differs significantly from the yearly average. The spider plots of Figs. 16 and 17 show how the cumulative distribution function changes from month to month. With only 3 years of Madrid data and 1 year of Goldstone data, it is not possible to discern between seasonal and yearly variations in the atmospheric noise temperature. The accumulation of additional years of data will permit the development of meaningful monthly MTF and MTR statistics. These data will show the seasonal behavior of Ka-band and allow the examination of new operational playback strategies involving retransmission of missed data.

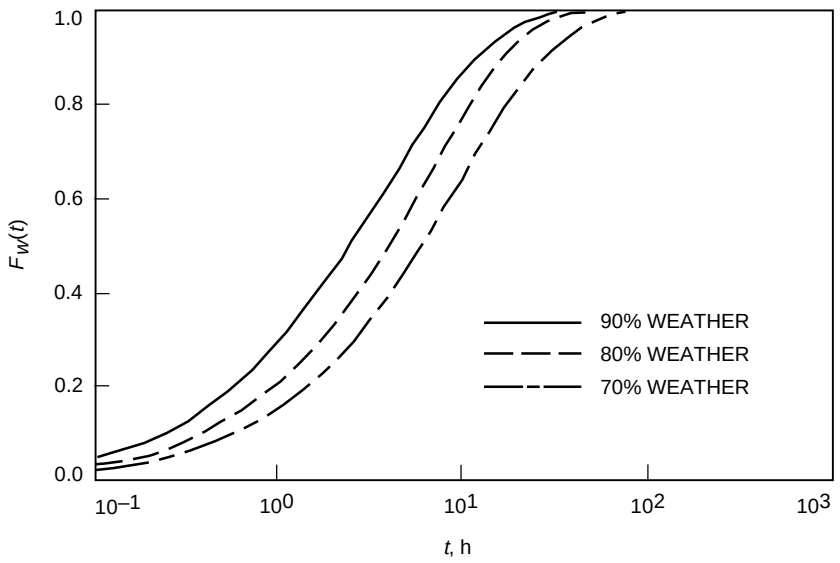

Fig. 15. Madrid weather link recovery.

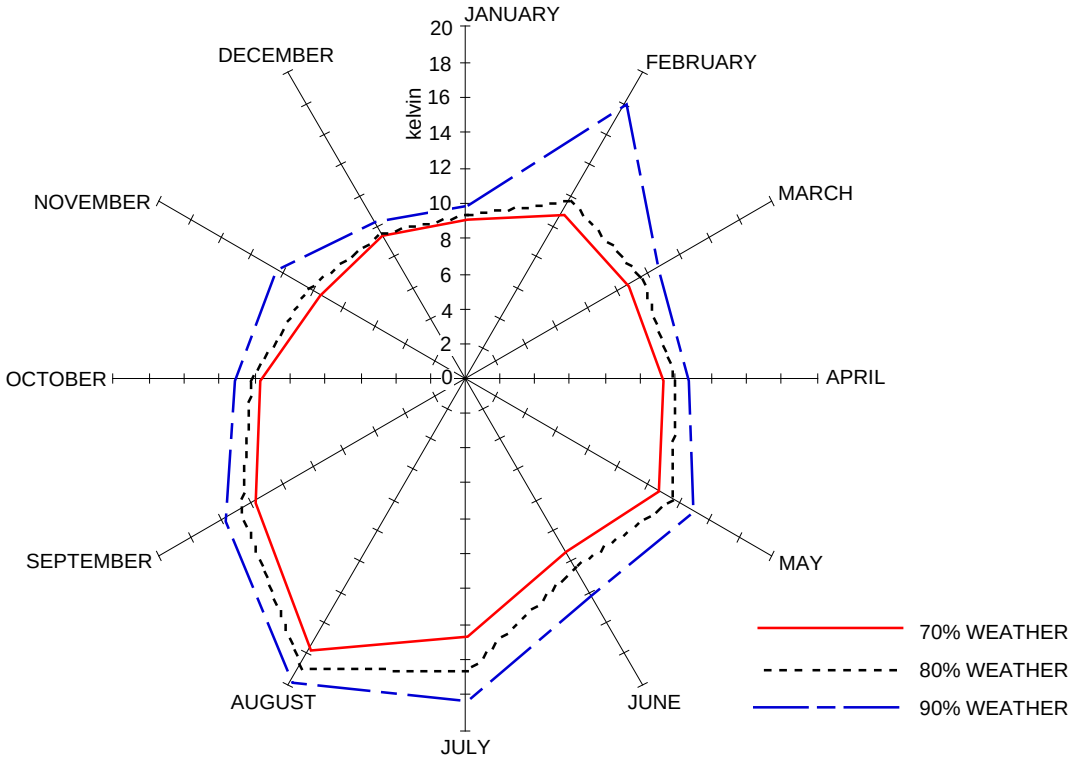

Fig. 16. Goldstone monthly atmospheric noise temperature: average monthly sky brightness temperature from October 1993 through September 1994 at a 90-deg elevation.

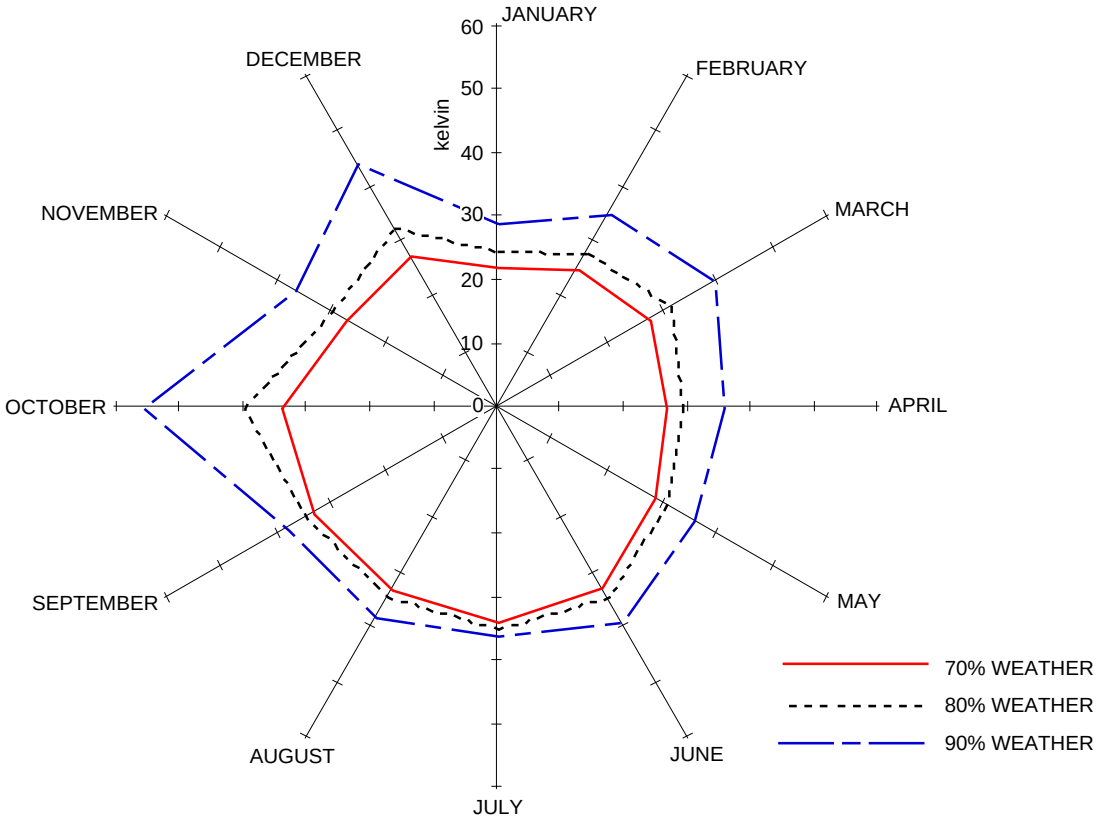

Fig. 17. Madrid monthly atmospheric noise temperature: average monthly sky brightness temperature from August 1990 through June 1993 at a 30-deg elevation.

Table 1. MTF and MTR weather statistics.

DSCC	Weather availability, percent	MTF, h	MTR, h
Goldstone	70	40.7	42.9
	80	58.5	42.9
	90	89.0	27.0
Madrid	70	26.5	10.7
	80	29.9	6.7
	90	38.2	4.6

The Microwave, Lidar, and Interferometer Technology Section is currently upgrading the water vapor radiometers at each DSN complex with real-time software to deliver automatically processed atmospheric noise temperature data to JPL via the Internet. As this system goes on-line, a computer workstation could be set up at JPL to receive the data from the WVRs and automatically generate MTF and MTR statistics on a monthly basis.

V. Conclusion

Applying renewal theory to Ka-band water vapor radiometer data increases our understanding of atmospheric effects on deep-space communications. In addition to standard weather availability percentages derived from cumulative distribution functions, mission planners now have a powerful tool to evaluate the mean time to failure and mean time to recovery for communication links designed to operate at a particular weather availability. Insight into this link behavior will lead to the development of new telemetry playback strategies for deep-space missions using Ka-band as their primary communication frequency.

Acknowledgments

The authors are grateful to S. Keihm and S. Slobin for their valuable technical insights and to T. McPheeters for computer programming support and assisting with the preparation of this manuscript.

References

[1] E. C. Posner, "Strategies for Weather-Dependent Data Acquisition," *The Telecommunications and Data Acquisition Progress Report 42-65, July–August 1981*, Jet Propulsion Laboratory, Pasadena, California, pp. 34–46, October 15, 1981.

[2] B. L. Gary, "Spain 31 GHz Observations of Sky Brightness Temperatures," *The Telecommunications and Data Acquisition Progress Report 42-94, April–June 1988*, Jet Propulsion Laboratory, Pasadena, California, pp. 42–60, August 15, 1988.

[3] B. L. Gary, "Australia 31 GHz Brightness Temperature Exceedance Statistics," *The Telecommunications and Data Acquisition Progress Report 42-94, April–June 1988*, Jet Propulsion Laboratory, Pasadena, California, pp. 61–74, August 15, 1988.

[4] A. Papoulis, *Probability, Random Variables, and Stochastic Processes*, third edition, New York: McGraw-Hill, Inc., 1991.